New method of estimating wavelength-dependent optical path length ratios for oxy- and deoxyhemoglobin measurement using near-infrared spectroscopy

Shinji Umeyama
Toru Yamada
Neuroscience Research Institute
National Institute of Advanced Industrial Science and Technology
Center 2, Umezono 1-1-1
Tsukuba, Ibaraki 305-8568
Japan
E-mail: s.umeyama@aist.go.jp

Abstract. In near-infrared spectroscopy (NIRS), concentration changes in oxy- and deoxyhemoglobin are calculated using an attenuation change of the measurement light and by solving a linear equation based on the modified Lambert-Beer law. While solving this equation, we need to know the wavelength-dependent mean optical path lengths of the measurement lights. However, it is very difficult to know these values by a continuous-wave-type (CW-type) system. We propose a new method of estimating wavelength-dependent optical path length ratios of the measurement lights based on the data obtained by a triple wavelength CW-type NIRS instrument. The proposed method does not give a path length itself, but it gives a path length ratio. Thus, it is possible to obtain the accurate hemoglobin concentration changes without cross talk, although the method cannot contribute to the quantification of the absolute magnitude of hemoglobin changes. The method is based on the principle that two possible estimations of hemoglobin concentration changes calculated using a triple-wavelength measurement system should be identical. The method was applied to the experimental data of human subjects' foreheads. The estimated path length ratios were very similar to literature values obtained by using picosecond laser pulses and a streak camera detector [M. Essenpreis et al., *Appl. Opt.* **32**(4), 418–425 (1993)].
 [DOI: 10.1117/1.3253350]

Keywords: near-infrared spectroscopy; wavelength-dependent mean optical path length; cross talk.

Paper 09171R received May 1, 2009; revised manuscript received Aug. 3, 2009; accepted for publication Aug. 21, 2009; published online Oct. 27, 2009.

1 Introduction

During functional brain activation, near-infrared spectroscopy (NIRS) is an effective tool for noninvasive investigation of cerebral oxygenation and hemodynamics.[1–3] It has several advantages over other functional measurement methods such as functional magnetic resonance imaging (fMRI), positron emission tomography (PET), and electroencephalogram (EEG). These advantages include good temporal resolution, measurement of both oxy- and deoxyhemoglobin (HbO and HbR), high portability, low restraints of subjects, and cost-effective equipment.[4] Several types of NIRS equipment are now available, such as time-resolved spectroscopy (TRS), phase-resolved spectroscopy (PRS), and continuous-wave-type (CW-type) instruments.

TRS-type and PRS-type instruments have some advantages over a CW-type instrument. For example, they can obtain mean optical path length of the measurement light, which can be used to realize a cross-talk-free hemoglobin concentration change estimation. However, since these instruments use a complex mechanism, they are usually more expensive than a CW-type instrument. On the other hand, the CW-type instrument is now very popular and widely used due to several practical reasons such as implementation cost. Thus, if we can estimate the mean optical path length ratio by using only CW-type measurement data, this contributes a realization of more accurate and reliable measurement of the CW-type instrument and should be very useful to many CW-type instrument users.

In a CW-type NIRS system, a simple calculation based on measuring the attenuation change of light as it propagates through a subject's head provides information about the concentration change of HbO and HbR in the brain. This calculation requires multiple measurement lights of different wavelengths, and the dual-or triple-wavelength measurement is widely used. The relationship between attenuation and concentration change is expressed using a linear equation based on the modified Lambert-Beer law. The coefficients in this equation include molar absorption coefficients of HbO and HbR and mean optical path lengths of the measurement light. All of these coefficients depend on the wavelength of the

Address all correspondence to: Shinji Umeyama, Neuroscience Research Institute, National Institute of Advanced Industrial Science and Technology, Center 2, Umezono 1-1-1, Tsukuba, Ibaraki 305-8568, Japan. Tel: 81 29-861-5837; Fax: 81 29-861-5841; E-mail: s.umeyama@aist.go.jp

1083-3668/2009/14(5)/054038/6/$25.00 © 2009 SPIE

measurement light. The molar absorption coefficients of HbO and HbR have been reported earlier.[5] On the other hand, the mean optical path lengths are difficult to determine using a CW-type instrument.

If the mean optical path length is not known, we cannot quantify hemoglobin concentration changes, and comparisons of NIRS measurements of different subjects and/or regions within a subject are impossible since the mean optical path length depends on subjects and a measured region within a subject. The mean optical path length depends also on the wavelength of the measurement light. Thus, if we do not know path lengths of used wavelengths, and substitute, for example, a wavelength-independent constant for these values, it inevitably introduces a source of error while calculating concentration changes. These errors are referred to as cross talk, because a change in one of the chromophores may mimic a change in the other chromophore.[6,7]

Since it is difficult to determine the mean optical path lengths using a CW-type instrument, they were usually measured by a TRS or PRS instrument beforehand,[8] or literature values[9–11] were substituted for these values.[12] In the former case, an additional TRS or PRS instrument is necessary, and these are usually more expensive than a CW-type instrument. In the latter case, the substituted values may be different from the true value since the path length depends on a subject and a measured region. Thus, if we have a method to estimate the path length only by a CW-type instrument, it could be useful to obtain the more accurate hemoglobin changes.

In this paper, we assume a triple-wavelength $(\lambda_1,\lambda_2,\lambda_3)$ measurement system and propose a new method for estimating the wavelength dependence of the mean optical path length. Here, we assume that only HbO and HbR contribute toward measured attenuation changes and that their concentrations change homogeneously in the tissue volume sampled by the detector. We also assume that optical path length does not change during a measurement.

Since two measurement lights with different wavelengths are sufficient to estimate two chromophores (HbO and HbR), two estimations of hemoglobin concentration changes can be obtained if we use a triple-wavelength measurement system—one calculated from data obtained using measurement lights λ_1 and λ_2 and the other from lights λ_2 and λ_3. Theoretically, these estimations should be identical; however, they are generally not identical if we assume $l(\lambda_1)=l(\lambda_2)=l(\lambda_3)$ in the calculation, where $l(\lambda_1)$, $l(\lambda_2)$, and $l(\lambda_3)$ are the mean optical path lengths of three wavelengths. The proposed method estimates optical path length ratios, $l(\lambda_2)/l(\lambda_1)$ and $l(\lambda_3)/l(\lambda_1)$, by minimizing squared differences of these two estimations. It cannot provide the absolute value of a mean optical path length; therefore, the absolute values of hemoglobin concentration changes are not obtained, and the method does not lead to the comparisons of NIRS measurements of different subjects and/or regions within a subject. However, accurate hemoglobin concentration changes free from cross talk with an arbitrary scaling can be obtained by the method.

There have been several studies on the wavelength-dependent optical path length estimation. Kahl et al. reported an estimation algorithm based on the assumption that the pulselike heartbeat response in observed absorbance changes are induced by volume changes in the arterial blood, which is saturated with oxygen.[13] Sakaguchi et al. estimated the wavelength dependence of mean optical path length at the exposed cortex of animals based on the same principle[14] as ours. However, their method did not take into account the measurement noise. Our simulation shown in this paper indicates that measurement noise significantly influences the estimation accuracy. We propose in this paper a new estimation method that provides an accurate estimation even with a relatively high noise level. The proposed method works without knowing a noise level. We think that this an important aspect of practical estimation, because sometimes the signal-to-noise ratio (SNR) of NIRS measurements of the human head is very low.

2 Theory

When a uniformly turbid medium is irradiated with near-infrared light, a temporal absorbance change ΔA resulting from a small homogeneous change in the absorption coefficient $\Delta\mu_a$ can be represented by using the modified Lambert-Beer law:

$$\Delta A(i,\lambda) = l(\lambda)\Delta\mu_a(i,\lambda) + n(i,\lambda), \tag{1}$$

where i is the sampling index, $l(\lambda)$ is the mean optical path length at wavelength λ, and $n(i,\lambda)$ is a measurement noise. The absorption coefficient change $\Delta\mu_a$ is given as

$$\Delta\mu_a(i,\lambda) = \varepsilon_{\mathrm{HbO}}(\lambda)\Delta\mathrm{HbO}(i) + \varepsilon_{\mathrm{HbR}}(\lambda)\Delta\mathrm{HbR}(i), \tag{2}$$

where ΔHbO and ΔHbR are oxy- and deoxyhemoglobin concentration changes, and $\varepsilon_{\mathrm{HbO}}$ and $\varepsilon_{\mathrm{HbR}}$ are their molar absorption coefficients, respectively.

The triple-wavelength measurement employs three light sources. If we use a vector representation of temporal attenuation changes, hemoglobin concentration changes, and measurement noises as

$$\boldsymbol{a_i} = [\Delta A(i,\lambda_1),\Delta A(i,\lambda_2),\Delta A(i,\lambda_3)]^T, \tag{3}$$

$$\boldsymbol{x_i} = [\Delta\mathrm{HbO}(i),\Delta\mathrm{HbR}(i)]^T, \tag{4}$$

$$\boldsymbol{n_i} = [n(i,\lambda_1),n(i,\lambda_2),n(i,\lambda_3)]^T. \tag{5}$$

Equations (1) and (2) are summarized as follows:

$$\boldsymbol{a_i} = LE\boldsymbol{x_i} + \boldsymbol{n_i}, \tag{6}$$

where

$$L = \mathrm{diag}[l(\lambda_1),l(\lambda_2),l(\lambda_3)], \tag{7}$$

$$E = \begin{bmatrix} \varepsilon_{\mathrm{HbO}}(\lambda_1) & \varepsilon_{\mathrm{HbR}}(\lambda_1) \\ \varepsilon_{\mathrm{HbO}}(\lambda_2) & \varepsilon_{\mathrm{HbR}}(\lambda_2) \\ \varepsilon_{\mathrm{HbO}}(\lambda_3) & \varepsilon_{\mathrm{HbR}}(\lambda_3) \end{bmatrix}. \tag{8}$$

We deduce the following equation by subtracting the average of each variable:

$$\tilde{\boldsymbol{a}}_i = LE\tilde{\boldsymbol{x}}_i + \tilde{\boldsymbol{n}}_i, \tag{9}$$

where

$$\tilde{\boldsymbol{a}}_i = \boldsymbol{a}_i - \bar{\boldsymbol{a}}, \tag{10}$$

$$\tilde{\boldsymbol{x}}_i = \boldsymbol{x}_i - \bar{\boldsymbol{x}}, \tag{11}$$

$$\tilde{\boldsymbol{n}}_i = \boldsymbol{n}_i - \bar{\boldsymbol{n}}. \tag{12}$$

Here, we calculate two estimations of temporal concentration changes. The first is calculated using the temporal absorbance change observed using wavelengths λ_1 and λ_2, and the second is calculated using wavelengths λ_2 and λ_3. These estimations should coincide with each other except for the noise, if we can correctly predict the unknown path length matrix L. If we write

$$\begin{bmatrix} \varepsilon_{\mathrm{HbO}}(\lambda_1) & \varepsilon_{\mathrm{HbR}}(\lambda_1) \\ \varepsilon_{\mathrm{HbO}}(\lambda_2) & \varepsilon_{\mathrm{HbR}}(\lambda_2) \end{bmatrix}^{-1} = \begin{pmatrix} u_{11} & u_{12} \\ u_{21} & u_{22} \end{pmatrix}, \tag{13}$$

$$\begin{bmatrix} \varepsilon_{\mathrm{HbO}}(\lambda_2) & \varepsilon_{\mathrm{HbR}}(\lambda_2) \\ \varepsilon_{\mathrm{HbO}}(\lambda_3) & \varepsilon_{\mathrm{HbR}}(\lambda_3) \end{bmatrix}^{-1} = \begin{pmatrix} v_{11} & v_{12} \\ v_{21} & v_{22} \end{pmatrix}, \tag{14}$$

two estimations are given as follows:

$$\boldsymbol{y}_i = U\hat{L}^{-1}\tilde{\boldsymbol{a}}_i, \tag{15}$$

$$\boldsymbol{z}_i = V\hat{L}^{-1}\tilde{\boldsymbol{a}}_i, \tag{16}$$

where

$$U = \begin{pmatrix} u_{11} & u_{12} & 0 \\ u_{21} & u_{22} & 0 \end{pmatrix}, \tag{17}$$

$$V = \begin{pmatrix} 0 & v_{11} & v_{12} \\ 0 & v_{21} & v_{22} \end{pmatrix}, \tag{18}$$

and $\hat{L}$ is a predicted matrix of L,

$$\hat{L} = \mathrm{diag}[\hat{l}(\lambda_1), \hat{l}(\lambda_2), \hat{l}(\lambda_3)]. \tag{19}$$

We assume that $\|\hat{L}\| = 1$, since we cannot estimate their absolute values. Thus, hemoglobin concentration change has an ambiguity in its scaling in our method.

If we can correctly predict the path length matrix L, two estimations should be identical. Thus, we can give the following criterion $J(\hat{L})$.

$$J(\hat{L}) = \frac{1}{N}\sum_{i=1}^{N} \|\boldsymbol{y}_i - \boldsymbol{z}_i\|^2. \tag{20}$$

By minimizing this criterion, an estimation of $\hat{L}$ is given. If there is no measurement noise ($\tilde{\boldsymbol{n}}_i = 0$), the obtained estimation is coincident with the true value except for its scaling. However, if there exists a noise, it has a kind of bias, and it is not coincident with the true value. In the following, we explain this and give an improved algorithm to solve this problem.

Using Eq. (9), $\boldsymbol{y}_i$ and $\boldsymbol{z}_i$ are represented as follows:

$$\boldsymbol{y}_i = U_1\tilde{\boldsymbol{x}}_i + U_2\tilde{\boldsymbol{n}}_i, \tag{21}$$

$$\boldsymbol{z}_i = V_1\tilde{\boldsymbol{x}}_i + V_2\tilde{\boldsymbol{n}}_i, \tag{22}$$

where

$$U_1 = U\hat{L}^{-1}LE, \quad U_2 = U\hat{L}^{-1}, \tag{23}$$

$$V_1 = V\hat{L}^{-1}LE, \quad V_2 = V\hat{L}^{-1}. \tag{24}$$

Thus, the criterion $J(\hat{L})$ is transformed as follows:

$$J(\hat{L}) = \frac{1}{N}\sum_{i=1}^{N} \|(U_1 - V_1)\tilde{\boldsymbol{x}}_i + (U_2 - V_2)\tilde{\boldsymbol{n}}_i\|^2, \tag{25}$$

$$\begin{aligned} &= \mathrm{tr}\{(U_1 - V_1)\Sigma_{xx}(U_1 - V_1)^T\} + 2\mathrm{tr}\{(U_1 - V_1)\Sigma_{xn}(U_2 - V_2)^T\} \\ &\quad + \mathrm{tr}\{(U_2 - V_2)\Sigma_{nn}(U_2 - V_2)^T\}, \end{aligned} \tag{26}$$

where Σ_{xx} and Σ_{nn} are covariance matrices of $\tilde{\boldsymbol{x}}$ and $\tilde{\boldsymbol{n}}$, respectively, and Σ_{xn} is their cross-covariance matrix. We assume that $\tilde{\boldsymbol{x}}$ and $\tilde{\boldsymbol{n}}$ are independent and also assume that $\Sigma_{nn} = \sigma_n^2 I$. Then,

$$J(\hat{L}) = \mathrm{tr}\{(U_1 - V_1)\Sigma_{xx}(U_1 - V_1)^T\} + \sigma_n^2\|U_2 - V_2\|^2. \tag{27}$$

If $\hat{L} = L/d$, where $d = \|L\|$, we have $U_1 = V_1 = dI$, and the first term of Eq. (27) becomes zero. Thus, the criterion $J(\hat{L})$ achieves its minimum value when $\hat{L} = L/d$ if no noise exists ($\sigma_n = 0$). However, since the second term of Eq. (27) works as a bias of the criterion if noise does exist, $\hat{L}$ that minimizes $J(\hat{L})$ is different from L/d. To avoid this difficulty, we propose the following criterion $J'(\hat{L})$:

$$J'(\hat{L}) = \frac{J(\hat{L})}{\|U_2 - V_2\|^2}. \tag{28}$$

Since $J'(\hat{L})$ is represented as follows from Eq. (27), the minimum of $J'(\hat{L})$ is achieved when $\hat{L} = L/d$ even if the magnitude σ_n of the noise is not zero:

$$J'(\hat{L}) = \frac{\mathrm{tr}\{(U_1 - V_1)\Sigma_{xx}(U_1 - V_1)^T\}}{\|U_2 - V_2\|^2} + \sigma_n^2. \tag{29}$$

The estimation process is a nonlinear optimization problem, and a MATLAB routine "iminsearch" was used to solve this problem. An initial value of the minimization process was set to be $\hat{L} = 0.5773I$ ($\|\hat{L}\| = 1$) in the following experiments. The convergence of the minimization was fast. For example, the computation time of an experiment in Sec. 3.2 was about 1 s by a PC (Core2 Duo 2.4 GHz).

3 Method

3.1 *Simulation of Path Length Estimation*

We give here a simple simulation of the proposed path length estimation method on artificial data to show the effectiveness

Fig. 1 Standard probes of a near-infrared oximeter, NIRO-200, attached on the left and right sides of a subject's forehead.

of the algorithm. The artificial data used in the simulation was prepared as follows. Real observed data of oxy- and deoxyhemoglobin concentration changes, which were calculated from the NIRS measurement data of 3600 samples of an adult forehead by using an ordinary estimation algorithm of modified Lambert-Beer law, were used for the hemoglobin concentration change $\boldsymbol{x}_i$. Then, $\boldsymbol{x}_i$ was transformed into the temporal absorbance change $\boldsymbol{a}_i$ as follows:

$$\boldsymbol{a}_i = L E \boldsymbol{x}_i + \boldsymbol{n}_i, \tag{30}$$

where E is given by assuming the wavelengths of three light sources are 776, 809, and 850 nm (λ_1, λ_2, λ_3, in this order), and L is assumed to be diag(1.0, 0.9, 0.8).

Noises were assumed to be mutually independent Gaussian noises with a zero mean. The noise variance σ_n^2 was defined as follows to give several SNR levels:

$$\mathrm{SNR} = 10 \log_{10} \frac{\text{mean variance of } LE\boldsymbol{x}}{\sigma_n^2}. \tag{31}$$

The optical path length estimations were performed by two methods: the simple method using the criterion J of Eq. (20), and the proposed method using the criterion J' of Eq. (28). For each SNR level, 50 different noise sequences were generated, and path length estimations were performed on these data. The average and the standard deviation of estimated optical path length ratios, $l(\hat{\lambda}_2)/l(\hat{\lambda}_1)$ and $l(\hat{\lambda}_3)/l(\hat{\lambda}_1)$, were calculated.

3.2 *Path Length Estimation by Experimental NIRS Data*

To prove the validity of our theoretical considerations, we tested the proposed path length estimation method by applying it to real data of NIRS measurements. We used a near-infrared oximeter (NIRO-200, Hamamatsu Photonics) and its standard probes. The probes are attached on the right and left sides of a subject's forehead (see Fig. 1). Each probe has two detectors of different source–detector distances (36 and 42 mm) to realize a spatially resolved spectroscopy (SRS). The subject sat still on a chair, and temporal absorbance changes were recorded for 10 min. Two healthy volunteers participated in the experiment. This study was approved by the Institutional Review Board of AIST, and the participants gave a written informed consent. The measurement sampling frequency was set at 6 Hz for 3600 samples. Three light sources with wavelengths of 776, 809, and 850 nm (λ_1, λ_2, λ_3, in this order) were used. Very low frequency components ($f < 0.005$ Hz) of the observed data were removed by fast Fourier transform (FFT) to eliminate the drift. Data recorded

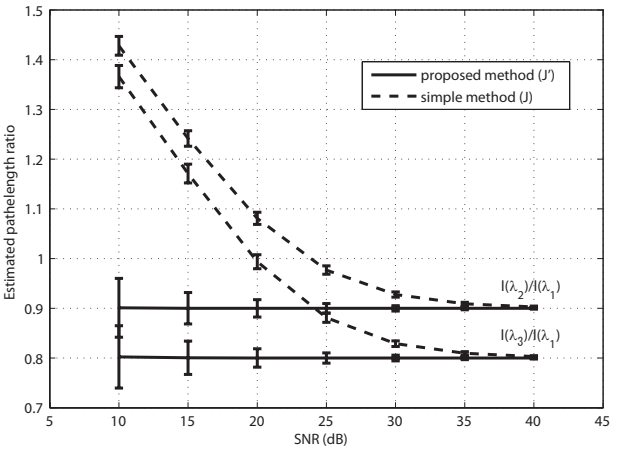

Fig. 2 Simulation results of mean optical path length ratio estimation. The true ratios, $l(\lambda_2)/l(\lambda_1)$ and $l(\lambda_3)/l(\lambda_1)$, were assumed as 0.9 and 0.8. On average, the solid and dashed lines show path length ratios estimated by the proposed method (J') and the simple method (J), respectively. Error bars represent the standard deviation of the estimations.

in the initial and final two minutes of the analysis were not used in calculation to avoid side-effects of low-frequency elimination. As a result, only 2160 samples were used in the estimation.

We applied two pathlength estimation methods—the proposed method based on criterion J' and the simple method based on criterion J—to the obtained NIRS data.

4 Results and Discussion

The simulation results are shown in Fig. 2. This figure shows that the simple method can give correct path length estimations only with a very high SNR. On the other hand, on average, the proposed method gives very accurate estimations even with a low SNR. The figure also indicates, however, that standard deviations of the estimated value distribution of the proposed method are not small with a low SNR. Thus, the estimated values widely vary around the average value when SNR is very low. Thus, in this case, the proposed method may fail to give accurate path length estimation, although it still gives better results than the simple method. To overcome this problem, we may need more data samples.

The estimated mean optical path length ratios calculated using the experimental data of NIRS measurement at the right and left side of the human subject's forehead are shown in Table 1. Since the probe used in the experiment has two detectors with their respective separation distances being 36 and 42 nm from the source, the estimated ratios for both detectors are shown in the table. Table 1 shows that the estimated ratios, $l(\lambda_2)/l(\lambda_1)$ and $l(\lambda_3)/l(\lambda_1)$, of the proposed method were approximately 0.94 and 0.83.

Essenpreis et al.[9] gave mean optical path lengths for wavelengths ranging from 740 to 840 nm by using picosecond laser pulses and a streak camera detector. The source–detector separation was 40 mm. Table 2 summarizes the mean optical path lengths of seven subjects for the three wavelengths (776, 809, and 850 nm) based on Fig. 4(a) of the Essenpreis report. Since the mean optical path length at wavelength 850 nm was

Table 1 Estimated mean optical path length ratios at the left and right forehead of a human subject.

Source–detector distance 36 mm					
		Proposed method (J')		Simple method (J)	
		$l(\lambda_2)/l(\lambda_1)$	$l(\lambda_3)/l(\lambda_1)$	$l(\lambda_2)/l(\lambda_1)$	$l(\lambda_3)/l(\lambda_1)$
Subject 1	Left forehead	0.93	0.82	1.20	1.14
	Right forehead	0.97	0.85	1.27	1.20
Subject 2	Left forehead	0.91	0.78	1.34	1.23
	Right forehead	0.89	0.78	1.23	1.13
Source–detector distance 42 mm					
		Proposed method (J')		Simple method (J)	
		$l(\lambda_2)/l(\lambda_1)$	$l(\lambda_3)/l(\lambda_1)$	$l(\lambda_2)/l(\lambda_1)$	$l(\lambda_3)/l(\lambda_1)$
Subject 1	Left forehead	0.94	0.84	1.25	1.19
	Right forehead	0.99	0.86	1.34	1.26
Subject 2	Left forehead	0.91	0.79	1.15	1.04
	Right forehead	0.97	0.86	1.15	1.06

not mentioned in this report, this value was determined by extrapolating the other data. Path length ratios were calculated using these path lengths and are given in the right columns of Table 2. They are very similar to the estimated path length ratios in Table 1. Path length ratios estimated by the simple method are also given in the right columns of Table 1. All these values are greater than the path length ratios obtained by the proposed method. The differences between the corresponding values were approximately 0.3. This result agrees well with the simulation results (Fig. 2).

Figure 3 shows time course examples of calculated oxy- and deoxyhemoglobin concentration changes. These time courses form a part of the concentration changes at the left forehead of subject 1. Figures 3(a) and 3(b) show the oxy- and deoxyhemoglobin concentration changes calculated using the equal path length assumption $[l(\lambda_1)=l(\lambda_2)=l(\lambda_3)]$. The dark solid lines indicate concentration changes calculated using λ_1 and λ_2 measurement, while the gray solid lines are those obtained using λ_2 and λ_3. These time courses do not completely agree with each other, particularly in the deoxyhemoglobin change. Figures 3(c) and 3(d) show oxy- and deoxyhemoglobin concentration changes calculated by using path length ratios estimated by the proposed method. The dark and gray

Table 2 Measured mean optical path lengths and their ratios. These values were based on the report of Essenpreis et al. (Ref. 9). The mean optical path length at wavelength 850 nm indicated by an asterisk (*) mark was determined by extrapolating the other data because it is not mentioned in the report.

	Mean optical path length			Path length ratio	
Subject	$l(776)$	$l(809)$	$l(850)^*$	$l(809)/l(776)$	$l(850)/l(776)$
1	237	232	210	0.98	0.89
2	244	238	216	0.97	0.89
3	252	246	224	0.97	0.89
4	254	247	222	0.97	0.87
5	262	251	231	0.96	0.88
6	264	260	237	0.99	0.90
7	298	282	258	0.95	0.86

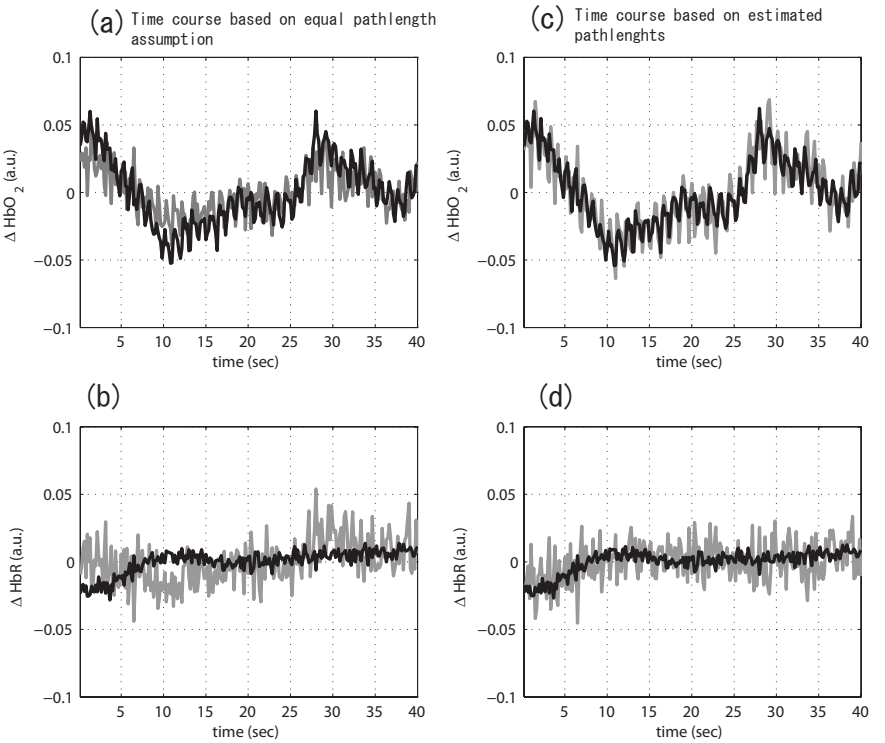

Fig. 3 Time course examples of calculated oxy- and deoxyhemoglobin concentration changes. These are a part of concentration changes at the left forehead of subject 1. Figures 3(a) and 3(b) show the oxy- and deoxyhemoglobin concentration changes calculated using the equal path length assumption $[l(\lambda_1)=l(\lambda_2)=l(\lambda_3)]$. Figures 3(c) and 3(d) show the same parameters calculated using estimated path length ratios. The dark solid lines indicate concentration changes calculated by λ_1 and λ_2 measurement, and the gray solid lines are those calculated by λ_2 and λ_3.

solid lines also indicate time courses by λ_1 and λ_2, and λ_2 and λ_3, respectively. These figures show that these two estimations agree very well with each other.

5 Conclusion

We propose a new method of estimating wavelength-dependent mean optical path length ratios of measurement lights. The method is based on the principle that two possible estimations of hemoglobin concentration changes calculated using triple-wavelength measurement system data should be identical. The proposed method was applied to the experimental data of human subjects' foreheads, and the estimated path length ratios were very similar to the literature values. The proposed method simply provides the ratio of path lengths and not their absolute values. The absolute value of the optical path length is required to compare observed responses at different positions.[8] Our method is not applicable to this problem. However, the proposed method estimates accurate hemoglobin concentration changes that are free from cross talk.

References

1. E. M. C. Hillman, "Optical brain imaging *in vivo*: techniques and applications from animal to man," *J. Biomed. Opt.* **12**(5), 051402 (2007).
2. Y. Hoshi, "Functional near-infrared spectroscopy: current status and future prospects," *J. Biomed. Opt.* **12**(6), 062106 (2007).
3. H. Obrig and A. Villringer, "Beyond the visible—imaging the human brain with light," *J. Cereb. Blood Flow Metab.* **23**, 1–18 (2003).
4. J. C. Hebden, "Advances in optical imaging of the newborn infant brain," *Psychophysiology* **40**, 501–510 (2003).
5. S. J. Matcher, C. E. Elwell, C. E. Cooper, M. Cope, and D. T. Delpy, "Performance comparison of several publishing tissue near-infrared spectroscopy algorithms," *Anal. Biochem.* **227**, 54–68 (1995).
6. K. Uludag, M. Kohl, J. Steinbrink, H. Obrig, and A. Villringer, "Cross talk in the Lambert-Beer calculation for near-infrared wavelengths estimated by Monte Carlo simulations," *J. Biomed. Opt.* **7**(1), 51–59 (2002).
7. G. Strangman, M. A. Franceschini, and D. A. Boas, "Factors affecting the accuracy of near-infrared spectroscopy concentration calculations for focal change in oxygenation parameters," *Neuroimage* **18**, 865–879 (2003).
8. Y. Hoshi, "Functional near-infrared optical imaging: utility and limitations in human brain mapping," *Psychophysiology* **40**, 511–520 (2003).
9. M. Essenpreis, C. E. Elwell, M. Cope, P. van der Zee, S. R. Arridge, and D. T. Delpy, "Spectral dependence of temporal point spread functions in human tissues," *Appl. Opt.* **32**(4), 418–425 (1993).
10. H. Zhao, Y. Tanikawa, F. Gao, Y. Onodera, A. Sassaroli, K. Tanaka, and Y. Yamada, "Maps of optical differential path length factor of human adult forehead, somatosensory motor, and occipital regions at multi-wavelengths in NIR," *Phys. Med. Biol.* **47**, 2075–2093 (2002).
11. A. Duncan, J. H. Meek, M. Clemence, C. E. Elwell, L. Tyszczuk, M. Cope, and D. T. Delpy, "Optical path length measurements on adult head, calf, and forearm and the head of the newborn infant using phase resolved optical spectroscopy," *Phys. Med. Biol.* **40**, 295–304 (1995).
12. M. A. Franceschini, S. Fantini, J. H. Thompson, J. P. Culver, and D. A. Boas, "Hemodynamic evoked response of the sensorimotor cortex measured noninvasively with near-infrared optical imaging," *Psychophysiology* **40**, 548–560 (2003).
13. M. Kahl, C. Nolte, H. R. Heekeren, S. Horst, U. Scholz, H. Obrig, and A. Villringer, "Determination of the wavelength dependence of the differential pathlength factor from near-infrared pulse signals," *Phys. Med. Biol.* **43**, 1771–1782 (1998).
14. K. Sakaguchi, T. Tachibana, S. Furukawa, T. Katsura, K. Yamazaki, H. Kawaguchi, A. Maki, and E. Okada, "Experimental prediction of the wavelength-dependent path-length factor for optical intrinsic signal analysis," *Appl. Opt.* **46**(14), 2769–2777 (2007).